Delineating antibody escape from Omicron sublineages

Henning Gruell[1,*], Kanika Vanshylla[1,*], Michael Korenkov[1], Pinkus Tober-Lau[2], Matthias Zehner[1], Friederike Münn[2], Hanna Janicki[1], Max Augustin[3], Philipp Schommers[1,3], Leif Erik Sander[2], Florian Kurth[2,4], Christoph Kreer[1], Florian Klein[1,5,6]

1 Laboratory of Experimental Immunology, Institute of Virology, Faculty of Medicine and University Hospital Cologne, University of Cologne, Cologne, Germany
2 Department of Infectious Diseases and Respiratory Medicine, Charité-Universitätsmedizin Berlin, Freie Universität Berlin and Humboldt-Universität zu Berlin, Berlin, Germany
3 Department I of Internal Medicine, Faculty of Medicine and University Hospital Cologne, University of Cologne, Cologne, Germany
4 Department of Tropical Medicine, Bernhard Nocht Institute for Tropical Medicine and Department of Medicine I, University Medical Center Hamburg-Eppendorf, Hamburg, Germany
5 German Center for Infection Research (DZIF), Partner site Bonn-Cologne, Cologne, Germany
6 Center for Molecular Medicine Cologne (CMMC), University of Cologne, Cologne, Germany
* These authors contributed equally

Correspondence should be addressed to florian.klein@uk-koeln.de.

Abstract

SARS-CoV-2 neutralizing antibodies play a critical role in prevention and treatment of COVID-19 but are challenged by viral evolution and antibody evasion, exemplified by the highly resistant Omicron BA.1 sublineage.[1-12] Importantly, the recently identified Omicron sublineages BA.2.12.1 and BA.4/5 with differing spike mutations are rapidly emerging in various countries. By determining polyclonal serum activity of 50 convalescent or vaccinated individuals against BA.1, BA.1.1, BA.2, BA.2.12.1, and BA.4/5, we reveal a further reduction of BA.4/5 susceptibility to vaccinee sera. Most notably, delineation of the sensitivity to an extended panel of 163 antibodies demonstrates pronounced antigenic differences of individual sublineages with distinct escape patterns and increased antibody resistance of BA.4/5 compared to the most prevalent BA.2 sublineage. These results suggest that the antigenic distance from BA.1 and the increased resistance compared to BA.2 may favor immune escape-mediated expansion of BA.4/5 after the first Omicron wave. Finally, while most monoclonal antibodies in clinical stages are inactive against all Omicron sublineages, we identify promising novel antibodies with high pan-Omicron neutralizing potency. Our study provides a detailed understanding of the antibody escape from the most recently emerging Omicron sublineages that can inform on effective strategies to prevent and treat COVID-19.

Main

Despite increasing levels of immunity against SARS-CoV-2 induced by vaccination and infection, the Omicron variant resulted in a global surge of infections that reflects its high transmissibility and immune evasion mediated by the highly mutated spike protein.[1,4-15] Although prolonged vaccine dosing intervals and booster immunizations based on the ancestral Wu01 strain elicit Omicron neutralizing serum activity, titers against Omicron

48 remain considerably lower compared to those against other variants.[4,6,11,16-18] Moreover,
49 the spike mutations of Omicron have rendered several therapeutic monoclonal antibodies
50 ineffective.[7,11,19] Most experimental evidence on the resistance of Omicron to antibody-
51 mediated neutralization is limited to analyses of the initial BA.1 strain. However, novel
52 sublineages are rapidly emerging and associated with increasing numbers of
53 infections.[20,21] Determining their antibody escape properties is therefore of critical
54 importance to effectively guide preventive and therapeutic measures. To this end, we
55 analyzed in detail antibody-mediated neutralization of prevalent and emerging Omicron
56 sublineages (BA.1, BA.1.1, BA.2, BA.2.12.1, and BA.4/5) both on a polyclonal and
57 monoclonal level.
58
59 **Results**
60
61 **Rapid spread of Omicron sublineages**
62 The spike protein of BA.1 differs in 39 amino acid residues from the ancestral Wu01 strain
63 of SARS-CoV-2 (**Fig. 1a**). While other Omicron sublineages share several mutations with
64 BA.1, they diverge at various amino acid positions including in critical antibody epitopes
65 (**Fig. 1a,b**). For example, the BA.1.1 spike protein contains an R346K substitution in the
66 receptor-binding domain (RBD) that was also observed in the SARS-CoV-2 Mu variant and
67 associated with escape from neutralizing antibodies (**Fig. 1a**).[22] While BA.1 and BA.1.1
68 dominated the initial Omicron surge, they were rapidly outcompeted by BA.2 (**Fig. 1c**).
69 BA.2 shares 21 of its 31 spike protein changes with BA.1 but differs considerably in both
70 the N-terminal domain (NTD) and the RBD, regions targeted by the most potent SARS-
71 CoV-2 neutralizing antibodies (**Fig. 1a,b**).

72 Following a decline in cases from the BA.1-/BA.2-related first Omicron wave, new
73 sublineages are rapidly emerging (**Fig. 1c**). For example, BA.2.12.1 outcompetes other
74 BA.2 sublineages in the United States resulting in an increase of infections. Moreover,
75 within weeks of their identification, the BA.4 and BA.5 sublineages with an identical spike
76 protein have become dominant in South Africa and Portugal and driven rising case
77 numbers (**Fig. 1c**).[21] BA.2.12.1 and BA.4/5 share the majority of their spike mutations
78 with BA.2 (94% and 90%, respectively), but contain additional changes at sites associated
79 with antibody escape. These include substitutions at residue 452 (L452Q in BA.2.12.1 and
80 L452R in BA.4/5, respectively) that were also recorded for the Lambda and Delta variants
81 (**Fig. 1a**).[23,24] In addition, the BA.4/5 spike protein harbors the F486V RBD mutation that
82 can reduce monoclonal antibody sensitivity but had not yet been observed in other
83 variants of interest or concern.[25] Thus, newly emerged Omicron sublineages differ from
84 BA.1 in key residues of the spike protein. Given their apparent growth advantages
85 compared to BA.1 and the prevalent BA.2, the sublineages BA.2.12.1 and BA.4/5 are likely
86 to be amongst the dominant variants of the SARS-CoV-2 pandemic in the near future.
87
88 **Reduced serum neutralizing activity against Omicron sublineages**
89 To determine Omicron sublineage escape profiles, we measured neutralizing activity
90 against the ancestral Wu01 strain as well as BA.1, BA.1.1, BA.2, BA.2.12.1, and BA.4/5
91 using lentivirus-based pseudovirus assays.[26,27] In order to assess escape from polyclonal
92 serum activity, we collected samples from two longitudinal cohorts of i.) SARS-CoV-2-
93 convalescent individuals (*n*=20) and ii.) vaccinated health care workers (*n*=30)
94 (**Extended Data Table 1**).[27,28] In both cohorts, individuals received an mRNA vaccine
95 booster immunization (BNT162b2) after a median of 14 months and 9 months following
96 infection or two doses of BNT162b2, respectively.

97 Convalescent individuals had a median age of 51 years (interquartile range [IQR]
98 35-60) and were diagnosed with mild or asymptomatic SARS-CoV-2 infection. All
99 individuals were infected during the initial phase of the pandemic between February and
100 April 2020, prior to the emergence of designated viral variants of concern. Early post-
101 infection samples (V1) were collected at a median of 48 days (IQR 34-58) after disease
102 onset or diagnosis and neutralizing activity was assessed by determining the 50%
103 inhibitory serum dilutions (ID_{50}s) (**Fig. 2a**). Neutralization of the Wu01 strain was
104 detected in all samples (100%) obtained early after infection, with individual ID_{50} values
105 ranging from 16 to 2,607 (geometric mean ID_{50} [GeoMeanID_{50}] of 264) (**Fig. 2b**). In
106 contrast, serum activity against Omicron sublineages was strongly reduced and only
107 detectable in 0-15% for BA.1 and BA1.1, and 45-50% for BA.2, BA.2.12.1, and BA.4/5 (**Fig.
108 2b**). However, analysis of sera obtained at a median of 33 days (IQR 27-54) after a single
109 BNT162b2 booster immunization revealed neutralizing activity against all tested
110 Omicron sublineages (**Fig. 2b, Extended Data Fig. 1a**) with GeoMeanID_{50}s ranging from
111 1,456 against BA.4/5 to 2,103 against BA.2 (**Fig. 2b, Extended Data Fig. 1b,c**).
112 In addition, we determined Omicron sublineage neutralizing activity induced
113 solely by vaccination (**Fig. 2c**). At a median of 28 days (IQR 27-32) after completion of the
114 initial two-dose course of BNT162b2 (V1), Wu01 neutralizing serum activity was detected
115 in all 30 individuals with a GeoMeanID_{50} of 561 (**Fig. 2d**). Although Omicron sublineage
116 neutralization was detectable in 43-73% of vaccinated individuals at V1, GeoMeanID_{50}s
117 were very low (ranging from 8-17) (**Fig. 2d**). Follow-up samples obtained at a median of
118 29 days (IQR 26-35) after booster immunization showed 8-fold higher activity against
119 Wu01 (GeoMeanID_{50} of 4,773) and strongly increased activity against all Omicron
120 sublineages (27- to 70-fold GeoMeanID_{50} increases) (**Fig. 2d, Extended Data Fig. 1d-f**).
121 Similar to the convalescent cohort, the lowest GeoMeanID_{50} after booster immunization

122 was observed against the BA.4/5 sublineages (GeoMeanID_{50} of 312, **Fig. 2d**). Of note,
123 amongst vaccinated individuals, the neutralizing activity against BA.4/5 was statistically
124 significantly lower compared to that against BA.1, BA.1.1, and BA.2 (GeoMeanID_{50}s of 648,
125 557, and 582, respectively) (**Extended Data Fig. 1e**).

126 We conclude that booster immunizations are critical to elicit neutralizing serum
127 activity against all prevalent Omicron sublineages in vaccinated as well as convalescent
128 individuals. Notably, BA.4/5 consistently demonstrated the lowest sensitivity of all
129 sublineages against polyclonal serum. These results suggest increased antigenic escape of
130 the recently emerged BA.4/5 sublineages mediated by the small number of spike protein
131 differences relative to BA.2.

132

133 **Dissecting escape of Omicron sublineages**

134 To decode Omicron escape from neutralizing antibodies on a molecular level, we
135 produced and tested 158 monoclonal antibodies isolated from SARS-CoV-2-convalescent
136 individuals against all sublineages. These included 67 randomly selected antibodies from
137 the Coronavirus Antibody Database (CoV-AbDab),[29] 79 antibodies isolated in our
138 previous work,[30,31] as well as 12 antibodies that were clinically tested. In total, this
139 antibody panel originated from at least 43 different individuals out of 19 independent
140 studies (**Fig. 3a**, **Extended Data Table 2**). All antibodies were identified in unvaccinated
141 individuals that were infected in the early phase of the pandemic prior to the emergence
142 of Omicron. The selection encompassed a broad spectrum of SARS-CoV-2 neutralizing
143 antibodies with 92 V_H/V_L combinations and a diverse range of CDR3 lengths and V gene
144 mutations (**Fig. 3a**, **Extended Data Table 2**). Most antibodies targeted the RBD (97%)
145 and the panel included previously described public clonotypes such as the V_H3-53/3-66
146 subgroup (**Fig. 3a**, **Extended Data Table 2**).

147 While all 158 antibodies neutralized the Wu01 strain, only 18%, 17%, 22%, 23%
148 and 18% remained active against BA.1, BA.1.1, BA.2, BA.2.12.1, and BA.4/5, respectively
149 (**Fig. 3b, Extended Data Fig. 2a, Extended Data Table 2**). Moreover, amongst antibodies
150 with retained neutralizing activity, the overall potency against Omicron sublineages was
151 6- to 14-fold lower compared to Wu01 with GeoMeanIC_{50}s of 0.42 (BA.1), 0.52 (BA.1.1),
152 0.17 (BA.2), 0.18 (BA.2.12.1), and 0.28 μg/ml (BA.4/5) (**Fig. 3c**).
153 The neutralization profiles revealed both commonalities and diversity in antibody
154 sensitivity of the different Omicron sublineages (**Fig. 3d-f, Extended Data Fig. 2b**).
155 Between the most closely related sublineages (BA.1 and BA.1.1; BA.2 and BA.2.12.1), only
156 small differences in antibody activity were observed (r_s of 0.81 and 0.86, respectively)
157 (**Fig. 3e,f Extended Data Fig. 2c**). In contrast, comparisons between the primary
158 sublineages BA.1, BA.2 and BA.4/5 demonstrated higher degrees of variation in antibody
159 susceptibility (**Fig. 3e,f**). For example, BA.2 was more resistant (>1 $\log_{10}$ IC_{50} difference)
160 than BA.1 to only a single antibody (2%), but more sensitive to ten antibodies (23%) (**Fig.
161 3e**). Moreover, higher fractions of antibodies showed >10-fold higher resistance against
162 BA.4/5 relative to other variants (**Fig. 3e**). While the comparison of BA.4/5 to BA.1 and
163 BA.1.1 revealed heterogeneity in sensitivity to the antibody panel with no correlation, the
164 sensitivity of BA.4/5 and BA.2 or BA.2.12.1 more strongly correlated (r_s of 0.58 and 0.68,
165 respectively). Importantly, however, whereas BA.4/5 were more sensitive to only 0-5%
166 of antibodies compared to BA.2 and BA.2.12.1, BA.4/5 showed higher resistance to 21%
167 of the antibodies (**Fig. 3e**).
168 Based on the analysis of the sublineage neutralization profiles, three prevalent
169 classes of Omicron neutralizing antibodies became apparent: i.) antibodies with broadly
170 comparable activity against Omicron sublineages (21/43, 49%), ii.) antibodies with
171 strongly reduced activity against BA.1 and BA.1.1 compared to BA.2, BA.2.12.1, and

172 BA.4/5 (7/43, 16%), and iii.) antibodies with strongly reduced activity against BA.4/5
173 compared to BA.1, BA.1.1, as well as BA.2 and/or BA.2.12.1 (6/43, 14%).
174 We conclude that in contrast to the limited differences in sensitivity to polyclonal
175 serum, Omicron sublineages considerably differ in their sensitivity to monoclonal
176 antibodies. Importantly, BA.4/5 demonstrated a strong bias to higher resistance
177 compared to the prevalent BA.2 sublineages.
178
179 **Minor sequence variations critically affect antibody activity**
180 Antibodies with Omicron neutralizing activity carried a modestly higher number of amino
181 acid mutations in the heavy and light chain variable gene compared to antibodies only
182 neutralizing Wu01 (median of 6 vs. 4 and 4 vs. 3 mutations; p=0.0143 and p=0.0170,
183 respectively), suggesting that higher sequence diversification might be overall favorable
184 for Omicron neutralization (**Fig. 3f, Extended Data Fig. 2e**).
185 Antibody responses against SARS-CoV-2 are highly convergent across individuals
186 based on the identification of public clonotypes with conserved sequence characteristics
187 and neutralization mechanisms.[32,33,34] Amongst the analyzed antibody panel, 18
188 sequences from 11 individuals could be assigned to the prominent V_H3-53/3-66|V_K1-9
189 clonotype (**Fig. 3g, Extended Data Fig. 2f**).[30,35,36] Although these antibodies are highly
190 conserved on a sequence level, they substantially differed in their Omicron neutralizing
191 capacity (**Fig. 3g, Extended Data Fig. 2f**). For example, antibodies R207-1C4 and R568-
192 2G5 harbor eight amino acid mutations in their V_H gene segment (without CDRH3) of
193 which five are at the same position and three are identical. While both antibodies had
194 similar Wu01 neutralizing activity, R207-1C4 did not neutralize any Omicron sublineage,
195 whereas R568-2G5 showed neutralizing activity against all variants. Notably, antibody

196 C140, another member of this clonotype which has the identical CDRH3 motif as R568-
197 2G5, did not neutralize any Omicron variant.
198 We conclude that minimal variation in antibody sequences can tip the scale
199 between Omicron neutralization and resistance. Thus, sequence- or antibody class-based
200 predictions of Omicron neutralization are difficult and experimental assessment of
201 individual monoclonal antibody activity remains essential.
202
203 **Impact on clinical and novel monoclonal antibodies**
204 SARS-CoV-2 neutralizing monoclonal antibodies can reduce morbidity and mortality in
205 infected individuals and are critical for passive immunization to protect individuals that
206 do not mount an adequate immune response upon vaccination.[2,3,37-41] To determine how
207 spike protein mutations of Omicron sublineages affect antibodies in clinical use, we
208 analyzed 9 monoclonal antibodies that received authorization for clinical use (**Fig. 4a,b**)
209 and 9 that are advanced in clinical development (**Fig. 4b, Extended Data Fig. 3**). All
210 antibodies target the RBD of the SARS-CoV-2 spike protein and were tested against Wu01
211 and the Omicron sublineages (**Fig. 4b**).
212 Most antibodies showed highly potent neutralizing activity against Wu01 with
213 IC_{50}s below 0.005 μg/ml (**Fig. 4b**). Less potent and incomplete Wu01 neutralizing activity
214 was observed for sotrovimab, consistent with previous reports showing reduced activity
215 against pseudoviruses lacking the dominant D614G spike mutation (**Fig. 4a**).[42,43] Only five
216 (28%) out of the 18 tested antibodies neutralized BA.1 with IC_{50}s <10 μg/ml, and of these,
217 three had strongly reduced potency (**Fig. 4b**). While the antibody neutralization profile of
218 BA.1.1 was generally similar to that of BA.1, there were some differences. For example,
219 DZIF-10c neutralized BA.1 with an IC_{50} of 0.046 μg/ml but completely lost activity against
220 BA.1.1 (**Fig. 4b, Extended Data Fig. 3**).

221 Although the number of antibodies in clinical use with neutralizing activity against
222 BA.2 (5 out 18, 28%), BA.2.12.1 (7 out 18, 39%), and BA.4/5 (6 out 18, 33%) was similarly
223 small, the neutralization profiles did differ (**Fig. 4b**). For example, cilgavimab neutralized
224 BA.2 and BA.2.12.1 with high potency (IC_{50}s of 0.008 and 0.014 μg/ml, respectively) but
225 was >480-fold less potent against BA.1 and BA.1.1 (**Fig. 4a,b**). While, cilgavimab
226 maintained high potency against BA.4/5 (IC_{50} of 0.085 μg/ml), the activity of antibody
227 DZIF-10c against BA.4/5 was strongly reduced when compared to BA.2 and BA.2.12.1
228 (8.64 vs. 0.03 μg/ml) (**Fig. 4b**). In contrast, whereas antibody imdevimab showed no
229 appreciable activity against BA.1 and BA.1.1, neutralization of BA.2, BA.2.12.1, and BA.4/5
230 was detectable at low levels (**Fig. 4a,b**).

231 Out of all clinical antibodies tested, only bebtelovimab maintained high
232 neutralization potency against all Omicron sublineages (IC_{50} <0.005 μg/ml; **Fig. 4a,b**). To
233 identify additional promising candidates, we examined antibodies previously isolated
234 from individuals with 'elite' IgG neutralizing activity.[30] Remarkably, antibodies R207-
235 2F11, R568-1G9, and R200-1F9 demonstrated highly potent neutralizing activity against
236 previously circulating variants (Wu01, B.1, Alpha, Beta, Delta, Epsilon, and Kappa), as well
237 as against BA.1, BA.1.1, BA.2, BA.2.12.1, and BA.4/5 with IC_{50}s <0.05 μg/ml (**Fig. 4d,**
238 **Extended Data Table 2**). These antibodies were identified from three different
239 convalescent individuals within weeks of infection during the early phase of the
240 pandemic.[30] Thus, the results highlight the capability of the immune system to generate
241 potent antibodies against the highly divergent Omicron variants in response to contact
242 with the ancestral spike protein.

243 We conclude that the prevalent and newly emerged Omicron sublineages,
244 including BA.2.12.1 and BA.4/5, escape from most monoclonal antibodies in clinical use.

245 Omicron sensitivity to these antibodies can, however, strongly differ on the sublineage
246 level.
247
248 **Discussion**
249 Antibody-mediated immunity is a critical component of prophylactic and therapeutic
250 measures against SARS-CoV-2 infection.[2,3,44,45] Throughout the COVID-19 pandemic, it has
251 however been confronted by the periodic emergence of antibody escape variants
252 developing in the context of increasing population immunity.[46] Omicron sublineages with
253 diverse spike proteins gaining prevalence suggest further increase in immune escape
254 and/or transmissibility.[20,21,47] Thus, establishing the impact of the recent BA.2.12.1 and
255 BA.4/5 sublineages on polyclonal and monoclonal immunity is critical to guide antibody-
256 mediated strategies for prevention and treatment.
257 Our results demonstrate that Wu01-based mRNA vaccine boosters are effective in
258 eliciting serum neutralizing activity against the diverse Omicron sublineages. However,
259 this activity is strongly limited compared to Wu01 neutralization and lower BA.4/5
260 neutralizing titers indicate even more pronounced immune evasion relative to previous
261 Omicron sublineages. Interestingly, the relative reduction in activity against BA.4/5 after
262 booster immunization was higher in infection-naïve than in convalescent individuals. This
263 might indicate differences in the breadth and potency of the neutralizing antibody
264 response elicited by infection only compared to those induced by "hybrid immunity".
265 While the differences in polyclonal serum sensitivity between the Omicron
266 sublineages were overall modest, our analysis of an extended antibody panel revealed
267 distinct patterns in sublineage sensitivity on a monoclonal level. Comparing Omicron
268 sublineages revealed the largest antigenic distance between BA.4/5 and BA.1/BA.1.1 as
269 indicated by the lack of correlation in antibody sensitivity and notable fractions of

270 antibodies showing higher sensitivity to one or the other sublineage. Whereas BA.4/5 and
271 BA.2/BA.2.12.1 showed more similar antibody susceptibility profiles, almost all
272 differences manifested as higher antibody resistance of BA.4/5.

273 Notably, minor differences in antibody sequence strongly affected Omicron
274 activity of antibodies with high potency against Wu01, highlighting the relative difficulty
275 of inducing antibodies with optimized Omicron neutralization after single contact with
276 Wu01-related spike. Accordingly and consistent with previous analyses on BA.1 and BA.2,
277 [48,49] almost all antibodies in clinical investigation showed strongly reduced or abolished
278 activity against all Omicron sublineages. However, we identify novel antibodies isolated
279 after ancestral infection with remarkable activity against all tested variants that may
280 provide options for immune-mediated treatment and prevention in the Omicron era of
281 the pandemic.

282 Our results suggest that outcompetition of BA.1(.1) by BA.2 may have been driven
283 mostly by higher transmissibility rather than by immune evasion. In contrast, higher
284 antigenic distance and antibody resistance of BA.4/5 may support its expansion after the
285 initial Omicron wave. The rapid emergence of Omicron sublineages with reduced
286 antibody susceptibility highlights the challenges posed by constant viral evolution and the
287 critical need for genomic surveillance and sensitivity assessments to inform on antibody-
288 based prophylactic and therapeutic measures.

289

290 **Acknowledgments**

291 We are grateful to all study participants for their dedication to our research. We thank F.
292 Dewald, L. Gieselmann, B. Kurt, C. Lehmann, P. Mayer, N. Riet, S. Salomon, M. Schlotz, R.
293 Schröder, R. Stumpf, and H. Wüstenberg, as well as the members of the EICOV/COVIM
294 Study Group (Y. Ahlgrimm, L. Bardtke, K. Behn, N. Bethke, H. Bias, D. Briesemeister, C.

295 Conrad, V. M. Corman, C. Dang-Heine, S. Dieckmann, C. Eroglu, D. Frey, J.-A. Gabelich, J.
296 Gerdes, U. Gläser, A. Hetey, L. Hasler, E. T. Helbig, D. Hillus, W. Hirst, A. Horn, C. Hülso, S.
297 Jentzsch, C. von Kalle, L. Kegel, A. Krannich, W. Koch, P. Kopankiewicz, P. Kroneberg, H. Le,
298 L. J. Lippert, C. Lüttke, P. de Macedo Gomes, B. Maeß, C. Matthaiou, J. Michel, A. Nitsche, A.-
299 M. Ollech, C. Peiser, A. Pioch, C. Pley, K. Pohl, C. Rubisch, L. Ruby, A. Sanchez Rezza, I.
300 Schellenberger, V. Schenkel, J. Schlesinger, S. Schmidt, G. Schwanitz, T. Schwarz, J. Seybold,
301 A. Solarek, A. Stege, S. Steinbrecher, P. Stubbemann, C. Thibeault, and D. Treue) for sample
302 acquisition and processing; L. Buchholz and M. Wunsch for help with antibody production
303 and preparation; and J.J. Malin for providing clinical antibody stocks. We thank all
304 laboratories obtaining and submitting SARS-CoV-2 sequencing information to GISAID for
305 facilitating rapid analyses of global variant distributions. This work was supported by
306 grants from COVIM: NaFoUniMedCovid19 (FKZ: 01KX2021) (to L.E.S. and F. Klein), the
307 Federal Institute for Drugs and Medical Devices (V-2021.3 / 1503_68403 / 2021–2022)
308 (to L.E.S. and F. Kurth), the German Center for Infection Research (DZIF) (to F. Klein), and
309 the Deutsche Forschungsgemeinschaft (DFG) CRC1310 (to C.K. and F. Klein).
310

311 **Author contributions**

312 Conceptualization, H.G., K.V., C.K., and F. Klein; methodology, H.G., K.V., L.E.S., F. Kurth, C.K.,
313 and F. Klein; investigation, H.G. and K.V.; resources, P.T-L., M.K., M.Z., F.M., H.J., M.A., and
314 P.S.; formal analysis, H.G., K.V., and C.K.; writing-original draft, H.G., K.V., C.K., and F. Klein;
315 writing-review and editing, M.K., P.T-L., and F. Kurth; visualization, H.G., K.V., C.K., and F.
316 Klein; supervision, L.E.S., F. Kurth, and F. Klein; funding acquisition, L.E.S., F. Kurth, and F.
317 Klein.
318
319

320 **Declaration of interests**

321 H.G., K.V., M.Z., C.K., and F. Klein are listed as inventors on patent applications on SARS-
322 CoV-2 neutralizing antibodies filed by the University of Cologne that encompass aspects
323 of this work.

324

325

326 **Figure legends**

327

328

329 **Fig. 1. Omicron sublineage differences.**

330 **a,** Spike amino acid changes in the BA.1, BA.1.1, BA.2, BA.2.12.1, and BA.4/5 Omicron
331 sublineages relative to Wu01. **b,** Locations of changed amino acids in Omicron sublineages
332 highlighted on the SARS-CoV-2 spike (PDB: 6XR8), with colors indicating mutations
333 shared between different sublineages. Representations at the bottom show RBD and NTD
334 outlined in black. Changes exclusive to BA.1.1 are indicated in green and those to BA.4/5
335 in brown, residue 452 (mutated in BA.2.12.1 and BA.4/5) is indicated in purple. **c,** Top
336 panels indicate weekly reported SARS-CoV-2 infections as aggregated by the COVID-19
337 Data Repository by the Center for Systems Science and Engineering at Johns Hopkins
338 University and http://ourworldindata.org. Relative proportions of infections by variant
339 per week were extrapolated from the proportion of sequences submitted to the GISAID
340 SARS-CoV-2 database per variant and week (accessed on May 24, 2022) shown in the
341 bottom panels. NTD, N-terminal domain; RBD, receptor-binding domain; PDB, Protein
342 Data Bank.

343

344

345 **Fig. 2. Omicron sublineage neutralizing serum activity in vaccinated and**
346 **convalescent individuals.**
347 **a,** Study scheme in COVID-19-convalescent individuals. Samples were collected after
348 infection occurring between February and April, 2020 (V1), and after a BNT162b2
349 booster immunization (V2). **b,** Fifty-percent inhibitory serum dilutions (ID_{50}s) against
350 Wu01, BA.1, BA.1.1, BA.2.12.1, and BA.4/5 determined by pseudovirus neutralization
351 assays in convalescent individuals. Bars indicate geometric mean ID_{50}s with 95%
352 confidence intervals (CIs) at V1 (left) and V2 (right). Numbers indicate geometric mean
353 ID_{50}s and percentage of individuals with detectable neutralizing activity (ID_{50} >10) in
354 parentheses. **c,** Study scheme in vaccinated individuals. Samples were collected after the
355 second dose of BNT162b2 (V1) and after the third dose of BNT162b2 (V2). **d,** Serum ID_{50}s
356 against Wu01, BA.1, BA.1.1, BA.2.12.1, and BA.4/5 determined by pseudovirus
357 neutralization assays in vaccinated individuals. Bars indicate geometric mean ID_{50}s with
358 95% CIs at V1 (left) and V2 (right). Numbers indicate geometric mean ID_{50}s and
359 percentage of individuals with detectable neutralizing activity (ID_{50} >10) in parentheses.
360 In **b** and **d**, ID_{50}s below the lower limit of quantification (LLOQ, ID_{50} of 10; indicated by
361 black dotted lines) were imputed to ½ LLOQ (ID_{50}=5), and ID_{50}s above the upper limit of
362 quantification (21,870) were imputed to 21,871.
363
364 **Fig. 3. Determining Omicron sublineage immune escape using monoclonal**
365 **antibodies.**
366 **a,** SARS-CoV-2 neutralizing monoclonal antibodies (*n*=158) derived from 19 studies and
367 ≥43 convalescent individuals were analyzed. Bar charts indicate number of antibodies per
368 heavy chain variable gene segment (V_H), amino acid (aa) length of the heavy chain
369 complementarity-determining region 3 (CDRH3), and number of V_H aa mutations relative

370 to the V_H germline gene. Pie chart indicates antibody epitopes with slice sizes proportional
371 to antibody fractions. RBD, receptor-binding domain. **b,** Fractions of antibodies from the
372 panel (*n*=158) displaying activity (IC_{50} <10 μg/ml) against Wu01 and Omicron
373 sublineages. **c,** IC_{50}s of neutralizing antibodies against individual variants/sublineages
374 (Wu01, *n*=158; BA.1, *n*=29; BA.1.1, *n*=27; BA.2, *n*=34; BA.2.12.1, *n=36*; BA.4/5, *n=29*). Solid
375 lines depict geometric mean IC_{50}s and 95% confidence intervals, and dashed lower and
376 upper lines indicate lower (LLOQ, 0.005 μg/ml) and upper limit of quantification (ULOQ,
377 10 μg/ml), respectively. IC_{50}s <LLOQ were imputed to ½ LLOQ (IC_{50}=0.0025). **d,** Heat map
378 depicting IC_{50}s of the subset of antibodies (*n*=43) with neutralizing activity (IC_{50} <10
379 μg/ml) against at least one of the Omicron sublineages. Antibodies are sorted based on
380 their potency against BA.1. **e,** Log_{10} IC_{50} ratios of antibodies neutralizing any Omicron
381 sublineage for indicated sublineage comparisons. Within each panel, antibodies are
382 sorted by increasing IC_{50} ratios. Ratios <-1 log_{10} are highlighted in green, ratios between
383 -1 and 1 log_{10} in grey, and ratios >1 log_{10} in red. Numbers indicate relative fractions. IC_{50}
384 <LLOQ were imputed to ½ LLOQ (IC_{50}=0.0025) and IC_{50} values >ULOQ were imputed to
385 2x ULOQ (IC_{50}=20). **f,** Spearman's rank correlation coefficients (rho) for comparisons of
386 antibodies with neutralizing capacity against any Omicron sublineage (*n*=43) as shown in
387 **Fig. S2c**. Numbers in bold indicate values with p<0.05. **g,** Heavy chain V amino acid
388 mutations of antibodies with neutralizing activity against Wu01 only and antibodies
389 neutralizing both Wu01 and at least one omicron sublineage. Lines indicate medians and
390 interquartile ranges. Groups were compared using the two-tailed Mann-Whitney U test.
391 **h,** Phylogenetic tree and heavy chain sequence alignment of antibodies of the V_H3-53/3-
392 66|V_K1-9 public clonotype. Letters indicate aa mutations relative to the V_H germline gene.
393 Number of aa mutations from corresponding germline allele and neutralizing activity
394 against Omicron sublineages are indicated on the right. Germline V_H represents the

395 consensus of all identified germline alleles of depicted antibodies (V_H3-53*01, V_H3-53*04,
396 and V_H3-66*01). Number of aa mutations from corresponding germline allele and
397 neutralizing activity against Wu01 and Omicron sublineages are indicated on the right.
398
399 **Fig. 4. Omicron sublineage neutralizing activity of monoclonal antibodies in clinical**
400 **use.**
401 **a,** Dose response curves showing percentage neutralization of monoclonal antibodies
402 against Wu01 and Omicron sublineages in pseudovirus neutralization assay. Circles show
403 averages and error bars indicate standard deviation. Dotted lines indicate 50%
404 neutralization (IC_{50}). **b,** IC_{50}s of monoclonal antibodies with current or previous
405 authorization for clinical use or in clinical development. Symbols indicate whether clinical
406 products or parental antibodies produced as human IgG1 were used. **c,** Dose response
407 curves showing percentage neutralization of novel monoclonal antibodies against Wu01
408 and Omicron sublineages in pseudovirus neutralization assay. Circles show averages and
409 error bars indicate standard deviation. Dotted lines indicate 50% neutralization (IC_{50}). **d,**
410 IC_{50}s of novel monoclonal antibodies shown in **c** against Wu01 and Omicron sublineages
411 (upper rows) and previously circulating variants (lower rows, as previously determined
412 [30]).
413
414 **Extended Data Figure legends**
415
416 **Extended Data Fig. 1. Serum neutralization of Omicron sublineages.**
417 **a,** Serum ID_{50}s against Wu01 and Omicron sublinages in the cohort of convalescent
418 individuals after infection (V1) and BNT162b2 booster immunization (V2) as in **Fig. 2**.
419 Lines connect ID_{50}s of individual participants at V1 and V2. Dashed lines indicate lower

420 limit of quantification (LLOQ, ID_{50}=10). **b,** Numbers in black indicate Spearman's rank
421 correlation coefficients (rho) for comparisons at V2 shown in **c**. Numbers in red indicate
422 *p* values determined by Friedman test followed by Dunn's multiple comparison test for
423 comparisons at V2, with statistically significant differences indicated in bold. **c,**
424 Correlation plots of log_{10} serum ID_{50}s against indicated viruses in convalescent
425 individuals at V2. **d,** Serum ID_{50}s against Wu01 and Omicron sublineages in the cohort of
426 BNT162b2-vaccinated individuals after the second (V1) and the third vaccine dose (V2)
427 as in **Fig. 2**. Lines connect ID_{50}s of individual participants at V1 and V2. Dashed lines
428 indicate lower limit of quantification (LLOQ, ID_{50}=10). **e,** Numbers in black indicate
429 Spearman's rank correlation coefficients (rho) for comparisons at V2 shown in **f**. Numbers
430 in red indicate *p* values determined by Friedman test followed by Dunn's multiple
431 comparison test for comparisons at V2, with statistically significant differences indicated
432 in bold. **f,** Correlation plots of log_{10} serum ID_{50}s against indicated viruses in vaccinated
433 individuals at V2. In **a** and **d**, Serum ID_{50}s <LLOQ were imputed to ½ LLOQ (ID_{50}=5).
434

435 **Extended Data Fig. 2. Neutralization profile of Omicron neutralizing antibodies.**
436 **a,** Spider plot of IC_{50}s for all antibodies against Wu01 and Omicron sublineages.
437 Antibodies are sorted arbitrarily but equally for each virus. Circles indicate IC_{50}s (from
438 outer to inner: 0.005, 0.05, 0.5, and 5 μg/ml). **b,** Bar charts of antibodies with neutralizing
439 activity (IC_{50} <10 μg/ml) against any Omicron sublineage (*n*=43). In each chart, antibodies
440 are sorted by BA.1-neutralizing activity. Dotted lines indicate lower (LLOQ, 0.005 μg/ml)
441 and upper limits of quantification (ULOQ; 10 μg/ml). **c,** IC_{50} correlation plots for
442 antibodies with neutralizing capacity against any Omicron sublineage (*n*=43). Colors
443 indicate epitopes as in **Fig. 3a**. Grey dashed lines represent identity lines and black dashed
444 lines indicate limits of quantification. In **a-c**, IC_{50}s <LLOQ were imputed to ½ LLOQ

445 (IC_{50}=0.0025) and IC_{50}s >ULOQ were imputed to 2x ULOQ (IC_{50}=20). **d,** Light chain V
446 amino acid mutations of antibodies with neutralizing activity against Wu01 only and
447 antibodies neutralizing both Wu01 and at least one omicron sublineage. Lines indicate
448 medians and interquartile ranges and groups were compared using the two-tailed Mann-
449 Whitney U test. **e,** Light chain sequence alignment of antibodies of the V_H3-53/3-66|V_K1-
450 9 public clonotype. Letters indicate amino acid (aa) mutations relative to the light chain
451 germline gene. Germline V_K represents the consensus of all identified germline alleles of
452 the depicted antibodies. Number of aa mutations from corresponding germline allele and
453 neutralizing activity against Wu01 and Omicron sublineages are indicated on the right.
454
455 **Extended Data Fig. 3. Omicron sublineage neutralizing activity of monoclonal**
456 **antibodies in clinical testing.**
457 Dose response curves showing % neutralization of monoclonal antibodies against Wu01
458 and Omicron sublineages in a pseudovirus neutralization assay. Circles show averages
459 and error bars indicate standard deviation. Dotted lines indicate 50% neutralization
460 (IC_{50}).
461
462 **Extended Data Tables**
463 **Extended Data Table 1**: Study cohorts
464 **Extended Data Table 2:** Monoclonal antibody panel analyses
465
466
467
468
469

470 **Methods**

471

472 **Study cohort and sample collection**

473 Serum samples from COVID-19-convalescent individuals were collected at the University
474 Hospital Cologne under study protocols approved by the ethics committee (EC) of the
475 Medical Faculty of the University of Cologne (16-054 and 20-1187). Between April and
476 May, 2020, individuals with a history of SARS-CoV-2 infection confirmed by polymerase
477 chain reaction (documented through a written test certificate or as reported to study
478 investigators by the participants) were enrolled within eight weeks of symptom onset
479 and/or diagnosis. As all participants were enrolled early during the pandemic (i.e., prior
480 to the emergence of variants of concern, as designated by the World Health Organization),
481 most individuals are likely to have been infected with an early viral strain similar to Wu01.
482 Participants were followed longitudinally to analyze long-term immunity to SARS-CoV-2.
483 Follow-up samples after booster immunization were collected between May and August,
484 2021. No additional SARS-CoV-2 infections between the sampling time points were
485 reported by any of the participants.

486 Serum samples from vaccinated individuals were collected under protocols
487 approved by the EC of Charité - Universitätsmedizin Berlin (EICOV, EA4/245/20) as well
488 as the EC of the Federal State of Berlin and the Paul Ehrlich Institute (COVIM, EudraCT-
489 No. 2021-001512-28). Study participation irrespective of medical conditions was offered
490 to health-care workers vaccinated at the Charité – Universitätsmedizin (Berlin, Germany).
491 All serum samples were tested for antibodies targeting the SARS-CoV-2 nucleocapsid
492 using the SeraSpot Anti-SARS-CoV-2 IgG microarray-based immunoassay (Seramun
493 Diagnostica). Samples from individuals with a history of SARS-CoV-2 infection, a positive
494 SARS-CoV-2 nucleic acid amplification test (performed at sampling), or detectable anti-

495 nucleocapsid antibodies were not included in this analysis. Serum samples after two
496 vaccinations were collected in February and March 2021 (for 29/30 participants; from
497 one participant, the early serum sample was obtained in July 2021); samples after booster
498 immunization were collected in December 2021 and January 2022.

499 All study participants provided written informed consent. Vaccinations in both
500 cohorts were performed as part of routine care outside of the observational studies.
501 Selection of participants and samples for analysis was based on receipt of identical
502 vaccines and comparable sampling time points relative to vaccinations. Serum samples
503 were collected after centrifugation and stored at -80°C until analysis.

504

505 **SARS-CoV-2 pseudovirus constructs**

506 All SARS-CoV-2 spike proteins were expressed using codon-optimized expression
507 plasmids. Wu01 (EPI_ISL_406716), BA.2.12.1, and BA.4/5 pseudoviruses were produced
508 using an expression plasmid that incorporated a C-terminal deletion of 21 cytoplasmic
509 amino acids that result in increased pseudovirus titers. Expression plasmids for Omicron
510 sublineage spike proteins were produced by assembling and cloning codon-optimized
511 overlapping gene fragments (Thermo Fisher) into the pCDNA3.1/V5-HisTOPO vector
512 (Thermo Fisher) using the NEBuilder HiFi DNA Assembly Kit (New England Biolabs), and
513 included the full spike protein amino acid sequences with the following amino acid
514 changes relative to Wu01:

515 BA.1: A67V, Δ69-70, T95I, G142D, Δ143-145, N211I, Δ212, ins215EPE, G339D, S371L,
516 S373P, S375F, K417N, N440K, G446S, S477N, T478K, E484A, Q493R, G496S, Q498R,
517 N501Y, Y505H, T547K, D614G, H655Y, N679K, P681H, N764K, D796Y, N856K, Q954H,
518 N969K, and L981F.

519 BA.1.1: As for BA.1 with an additional R346K mutation.

520 BA.2: T19I, Δ24-26, A27S, A67V, G142D, V213G, G339D, S371F, S373P, S375F, T376A,
521 D405N, R408S, K417N, N440K, S477N, T478K, E484A, Q493R, Q498R, N501Y, Y505H,
522 D614G, H655Y, N679K, P681H, N764K, D796Y, Q954H, N969K.
523 BA.2.12.1: As for BA.2 with additional L452Q and S704L mutations.
524 BA.4/5: As for BA.2 with additional Δ69-70, L452R, and F486V mutations, but lacking the
525 Q493R mutation.
526 All plasmid sequences were verified by sequencing.
527
528 **Monoclonal antibodies**
529 Monoclonal antibodies previously isolated in our lab had been obtained by single cell-
530 sorting of SARS-CoV-2 spike-specific B cells followed by reverse transcription, PCR
531 amplification and cloning of antibody variable regions.[30,31] For monoclonal antibodies
532 derived from the CoV-AbDab [29], variable region amino acid sequences were reverse
533 translated with the reverse translate tool from the Sequence Manipulation Suite[50] using
534 the *Homo sapiens* codon table obtained from the Codon Usage Database,[51] and sequences
535 were ordered as gene fragments from Integrated DNA Technologies (IDT) with 5' and 3'
536 overhangs. The variable regions were inserted into heavy and light chain expression
537 plasmids[52] by sequence- and ligation-independent cloning (SLIC). For antibodies ADG-2,
538 COV2-2130 (cilgavimab), COV2-2196 (tixagevimab), COV2-2381, MAD0004J08, and P2C-
539 1F11 (BRII-196), gene fragments based on the nucleotide sequences published in
540 GenBank were ordered at IDT and cloned as above. For antibodies C135, CT-P59
541 (regdanvimab), and LY-CoV1404 (bebtelovimab), gene fragments based on antibody
542 structures deposited in the Protein Data Bank (accession nos. 7K8Z, 7CM4, and 7MMO)
543 were ordered at IDT after codon optimization using the IDT Codon Optimization Tool and
544 cloned as above. For antibodies 47D11, BD-368-2, C144, and P2B-2F6, amino acid

545 sequences were derived from CoV-AbDaB, corresponding nucleotide sequences
546 generated and codon-optimized using the IDT Codon Optimization Tool, and gene
547 fragments cloned as above.

548 Monoclonal antibody production was performed using 293-6E cells (National
549 Research Council of Canada) by co-transfection of heavy and light chain expression
550 plasmids using 25 kDa branched polyethylenimine (Sigma-Aldrich). Culture supernatants
551 were harvested after an incubation period of 6-7 days at 37°C and 6% CO2 under constant
552 shaking in FreeStyle Expression Medium supplemented with penicillin (20 U/ml) and
553 streptomycin (20 µg/ml) (all Thermo Fisher). Clarified cell supernatants were incubated
554 with Protein G Sepharose 4 FastFlow (Cytiva) overnight at 4°C . After centrifugation,
555 antibodies bound to Protein G beads were eluted in chromatography columns (Bio-Rad)
556 using 0.1 M glycine (pH=3.0) and buffered in 1 M Tris (pH=8.0). Buffer exchange to PBS
557 was performed using centrifugal filter units (Millipore). For antibodies bamlanivimab,
558 casirivimab, DZIF-10c, etesevimab, imdevimab, and sotrovimab, aliquots from clinical
559 stocks were used.

560

561 **Pseudovirus neutralization assays**

562 Neutralization assays were performed using lentivirus-based pseudoviruses and ACE2-
563 expressing 293T cells.[26,27] Pseudovirus particle production was performed in HEK293T
564 cells by co-transfection of individual expression plasmids encoding for the SARS-CoV-2
565 spike protein, HIV-1 Tat, HIV-1 Gag/Pol, HIV-1 Rev, and luciferase-IRES-ZsGreen using
566 FuGENE 6 Transfection Reagent (Promega). Culture supernatants were exchanged with
567 fresh medium (high glucose DMEM supplemented with 2 mM L-glutamine, 100 IU/ml
568 penicillin, 100 µg/ml streptomycin, 1 mM sodium pyruvate (all Thermo Fisher), and 10%
569 FBS (Sigma-Aldrich)) 24 h post transfection. Pseudovirus-containing supernatants were

570 harvested between 48-72 h after transfection, centrifuged, clarified using a 0.45 µm filter,
571 and stored at -80°C. Pseudoviruses were titrated by infection of 293T-ACE2 cells and
572 luciferase activity was determined after a 48-hour incubation at 37°C and 5% CO_2 by
573 addition of luciferin/lysis buffer (10 mM $MgCl_2$, 0.3 mM ATP, 0.5 mM coenzyme A, 17 mM
574 IGEPAL CA-630 (all Sigma-Aldrich), and 1 mM D-Luciferin (GoldBio) in Tris-HCL) using a
575 microplate reader (Berthold).

576 Serum samples were heat-inactivated at 56°C for 45 min before use. Three-fold
577 serial dilutions of serum (starting at 1:10) and monoclonal antibodies (starting at 10
578 µg/ml) were prepared in culture medium and co-incubated with pseudovirus
579 supernatants for one hour at 37°C and 5% CO_2 prior to addition of 293T-ACE2 cells.
580 Following a 48-hour incubation at 37°C and 5% CO_2, luciferase activity was determined
581 as described above. Average background relative light units (RLUs) of non-infected cells
582 were subtracted, and serum ID_{50}s and antibody IC_{50}s were determined as the serum
583 dilutions and antibody concentrations resulting in a 50% RLU reduction compared to the
584 average of virus-infected untreated controls cells using a non-linear fit model plotting an
585 agonist vs. normalized dose response curve with variable slope using the least squares
586 fitting method in Prism 7.0 (GraphPad). All serum and monoclonal antibody samples were
587 tested in duplicates. Imputation rules for values outside the limits of quantification are
588 described below (see Statistical methods).

589

590 **SARS-CoV-2 neutralizing antibody panel and sequence analysis**

591 The panel of 158 SARS-CoV-2 neutralizing monoclonal antibodies isolated from SARS-
592 CoV-2 convalescent individuals included in the analysis in **Fig. 3** is based on 79 antibodies
593 obtained in our previous work,[30,31] 67 randomly selected (retrieved on January 1, 2021)
594 human SARS-CoV-2 neutralizing antibodies deposited at CoV-AbDab,[29] and 12 antibodies

595 in clinical use or development. We did not include five of the antibodies in clinical
596 development shown in **Fig. 4** into this analysis, as they were obtained from individuals
597 infected with SARS-CoV (ADG-2, sotrovimab), from immunized mice harboring human
598 immunglobulin gene repertoires (47D11, casirivimab), or using phage display technology
599 that does not ensure native pairing of antibody heavy and light chains (regdanvimab).

600 Antibody amino acid sequences were annotated with IgBLASTp[53] based on the
601 IMGT database.[54] For sequence statistics, top V gene calls were counted without
602 individual alleles, CDR3 lengths are reported according to the IMGT numbering system
603 and numbers of V mutations refer to the top V gene call from IgBLASTp. Phylogenetic
604 analysis of antibodies belonging to the V_H3-53/3-66|V_K1-9 public clonotype was
605 performed by alignment of amino acid sequences with the MAFFT algorithm[55] via the
606 EMBL-EBI search and sequence analysis tools API[56] and the Tree Builder tool from
607 Geneious Prime 2020.0.4 (Biomatters) using the Jukes-Cantor distance model for tree
608 building with the neighbour-joining method without resampling. Data aggregation and
609 visualization was performed with the Python libraries pandas (v1.1.5), NumPy (v1.19.2),
610 SciPy (v1.5.2), Matplotlib (v3.3.4) with Python (v3.6.8), as well as Microsoft Excel 2011
611 for Mac (v14.7.3), and Adobe Illustrator.

612

613 **Visualization of SARS-CoV-2 spike amino acid changes**

614 Amino acid changes relative to the Wu01 spike protein were visualized on a cryo-electron
615 microscopy 3D-reconstruction of the SARS-CoV-2 spike protein (PDB ID: 6XR8, ref. [57])
616 using ChimeraX (v. 1.3).[58,59]

617

618

619

620 **SARS-CoV-2 variant distribution**

621 Numbers of weekly cases as curated by the COVID-19 Data Repository by the Center for
622 Systems Science and Engineering (CSSE) at Johns Hopkins University[60] was retrieved
623 from http://ourworldindata.org (accessed on May 24, 2022). GISAID-curated clade and
624 lineage statistics of sequences submitted to the GISIAD database[61-63] were retrieved from
625 GISAID (accessed on May 24, 2022) and frequency of individual variants was plotted as
626 fraction of all submitted sequences per week and variant. For visualization, all BA.1
627 sublineages except for BA.1.1 (and sublineages of BA.1.1) were classified as BA.1, and all
628 BA.2 sublineages except for BA.2.12.1 were classified as BA.2

629

630 **Statistical Methods**

631 For graphical representation and statistical evaluation of serum samples in **Fig. 2** and
632 **Extended Data Fig. 1**, samples that did not achieve 50% inhibition at the lowest tested
633 dilution of 10 (lower limit of quantification, LLOQ) were imputed to ½ of the LLOQ
634 (ID_{50}=5) and serum samples with ID_{50} >21,870 (upper limit of quantification) were
635 imputed to ID_{50}=21,871. For graphical representation and statistical analysis of
636 monoclonal neutralizing antibodies in **Fig. 3** and **Extended Data Fig. 2**, IC_{50} values of
637 antibodies with an IC_{50} <0.005 μg/ml (LLOQ) were imputed to ½ LLOQ (IC_{50}=0.0025), and
638 IC_{50} values >10 μg/ml (ULOQ) were imputed to 2x ULOQ (IC_{50}=20 μg/ml).

639 Testing for statistical significance of differences in serum neutralization titers
640 against different variants/sublinages was performed with the Friedman test with Dunn's
641 multiple comparison using Prism 7.0 (GraphPad). Spearman's rank correlation
642 coefficients (Rho) were determined using Prism 7.0 (GraphPad). Amino acid mutations
643 relative to germline between antibodies neutralizing Wu01 only and those neutralizing

644 any Omicron sublineage were compared with two-sided Mann-Whitney U tests using
645 Prism 7.0 (GraphPad).
646

647 **Data and code availability**

648 Requests for data or materials should be directed to the corresponding author and may
649 be subject to restrictions based on data and privacy protection regulations and/or may
650 require a Material Transfer Agreement (MTA). The paper does not report original code.
651

652 **References**

653 1 Andrews, N. *et al.* Covid-19 Vaccine Effectiveness against the Omicron (B.1.1.529)
654 Variant. *N Engl J Med* **386**, 1532-1546, doi:10.1056/NEJMoa2119451 (2022).
655 2 Corti, D., Purcell, L. A., Snell, G. & Veesler, D. Tackling COVID-19 with neutralizing
656 monoclonal antibodies. *Cell* **184**, 3086-3108, doi:10.1016/j.cell.2021.05.005 (2021).
657 3 Gruell, H. *et al.* Antibody-Mediated Neutralization of SARS-CoV-2. *Immunity*,
658 doi:10.1016/j.immuni.2022.05.005 (2022).
659 4 Garcia-Beltran, W. F. *et al.* mRNA-based COVID-19 vaccine boosters induce
660 neutralizing immunity against SARS-CoV-2 Omicron variant. *Cell* **185**, 457-466 e454,
661 doi:10.1016/j.cell.2021.12.033 (2022).
662 5 Carreno, J. M. *et al.* Activity of convalescent and vaccine serum against SARS-CoV-2
663 Omicron. *Nature* **602**, 682-688, doi:10.1038/s41586-022-04399-5 (2022).
664 6 Schmidt, F. *et al.* Plasma Neutralization of the SARS-CoV-2 Omicron Variant. *N Engl J*
665 *Med* **386**, 599-601, doi:10.1056/NEJMc2119641 (2022).
666 7 Liu, L. *et al.* Striking antibody evasion manifested by the Omicron variant of SARS-
667 CoV-2. *Nature* **602**, 676-681, doi:10.1038/s41586-021-04388-0 (2022).
668 8 Planas, D. *et al.* Considerable escape of SARS-CoV-2 Omicron to antibody
669 neutralization. *Nature* **602**, 671-675, doi:10.1038/s41586-021-04389-z (2022).
670 9 Cele, S. *et al.* Omicron extensively but incompletely escapes Pfizer BNT162b2
671 neutralization. *Nature* **602**, 654-656, doi:10.1038/s41586-021-04387-1 (2022).
672 10 Hoffmann, M. *et al.* The Omicron variant is highly resistant against antibody-
673 mediated neutralization: Implications for control of the COVID-19 pandemic. *Cell* **185**,
674 447-456 e411, doi:10.1016/j.cell.2021.12.032 (2022).
675 11 Gruell, H. *et al.* mRNA booster immunization elicits potent neutralizing serum activity
676 against the SARS-CoV-2 Omicron variant. *Nat Med* **28**, 477-480, doi:10.1038/s41591-
677 021-01676-0 (2022).
678 12 Tseng, H. F. *et al.* Effectiveness of mRNA-1273 against SARS-CoV-2 Omicron and Delta
679 variants. *Nat Med*, doi:10.1038/s41591-022-01753-y (2022).
680 13 Altarawneh, H. N. *et al.* Protection against the Omicron Variant from Previous SARS-
681 CoV-2 Infection. *N Engl J Med* **386**, 1288-1290, doi:10.1056/NEJMc2200133 (2022).
682 14 Viana, R. *et al.* Rapid epidemic expansion of the SARS-CoV-2 Omicron variant in
683 southern Africa. *Nature* **603**, 679-686, doi:10.1038/s41586-022-04411-y (2022).

15 Madhi, S. A. *et al.* Population Immunity and Covid-19 Severity with Omicron Variant in South Africa. *N Engl J Med* **386**, 1314-1326, doi:10.1056/NEJMoa2119658 (2022).
16 Zhao, X. *et al.* Effects of a Prolonged Booster Interval on Neutralization of Omicron Variant. *N Engl J Med* **386**, 894-896, doi:10.1056/NEJMc2119426 (2022).
17 Wratil, P. R. *et al.* Three exposures to the spike protein of SARS-CoV-2 by either infection or vaccination elicit superior neutralizing immunity to all variants of concern. *Nat Med* **28**, 496-503, doi:10.1038/s41591-022-01715-4 (2022).
18 Perez-Then, E. *et al.* Neutralizing antibodies against the SARS-CoV-2 Delta and Omicron variants following heterologous CoronaVac plus BNT162b2 booster vaccination. *Nat Med* **28**, 481-485, doi:10.1038/s41591-022-01705-6 (2022).
19 VanBlargan, L. A. *et al.* An infectious SARS-CoV-2 B.1.1.529 Omicron virus escapes neutralization by therapeutic monoclonal antibodies. *Nat Med* **28**, 490-495, doi:10.1038/s41591-021-01678-y (2022).
20 Yamasoba, D. *et al.* Virological characteristics of the SARS-CoV-2 Omicron BA.2 spike. *Cell*, doi:10.1016/j.cell.2022.04.035 (2022).
21 Tegally, H. *et al.* Continued Emergence and Evolution of Omicron in South Africa: New BA.4 and BA.5 lineages. *medRxiv*, doi:10.1101/2022.05.01.22274406 (2022).
22 Greaney, A. J. *et al.* Mapping mutations to the SARS-CoV-2 RBD that escape binding by different classes of antibodies. *Nat Commun* **12**, 4196, doi:10.1038/s41467-021-24435-8 (2021).
23 Kimura, I. *et al.* The SARS-CoV-2 Lambda variant exhibits enhanced infectivity and immune resistance. *Cell Rep* **38**, 110218, doi:10.1016/j.celrep.2021.110218 (2022).
24 Planas, D. *et al.* Reduced sensitivity of SARS-CoV-2 variant Delta to antibody neutralization. *Nature* **596**, 276-280, doi:10.1038/s41586-021-03777-9 (2021).
25 Baum, A. *et al.* Antibody cocktail to SARS-CoV-2 spike protein prevents rapid mutational escape seen with individual antibodies. *Science* **369**, 1014-1018, doi:10.1126/science.abd0831 (2020).
26 Crawford, K. H. D. *et al.* Protocol and Reagents for Pseudotyping Lentiviral Particles with SARS-CoV-2 Spike Protein for Neutralization Assays. *Viruses* **12**, doi:10.3390/v12050513 (2020).
27 Vanshylla, K. *et al.* Kinetics and correlates of the neutralizing antibody response to SARS-CoV-2 infection in humans. *Cell Host Microbe* **29**, 917-929 e914, doi:10.1016/j.chom.2021.04.015 (2021).
28 Hillus, D. *et al.* Safety, reactogenicity, and immunogenicity of homologous and heterologous prime-boost immunisation with ChAdOx1 nCoV-19 and BNT162b2: a prospective cohort study. *The Lancet Respiratory Medicine* **9**, 1255-1265, doi:10.1016/s2213-2600(21)00357-x (2021).
29 Raybould, M. I. J., Kovaltsuk, A., Marks, C. & Deane, C. M. CoV-AbDab: the coronavirus antibody database. *Bioinformatics* **37**, 734-735, doi:10.1093/bioinformatics/btaa739 (2021).
30 Vanshylla, K. *et al.* Discovery of ultrapotent broadly neutralizing antibodies from SARS-CoV-2 elite neutralizers. *Cell Host Microbe* **30**, 69-82 e10, doi:10.1016/j.chom.2021.12.010 (2022).
31 Kreer, C. *et al.* Longitudinal Isolation of Potent Near-Germline SARS-CoV-2-Neutralizing Antibodies from COVID-19 Patients. *Cell* **182**, 843-854 e812, doi:10.1016/j.cell.2020.06.044 (2020).
32 Robbiani, D. F. *et al.* Convergent antibody responses to SARS-CoV-2 in convalescent individuals. *Nature* **584**, 437-442, doi:10.1038/s41586-020-2456-9 (2020).

732 33 Nielsen, S. C. A. *et al.* Human B Cell Clonal Expansion and Convergent Antibody
733 Responses to SARS-CoV-2. *Cell Host Microbe* **28**, 516-525 e515,
734 doi:10.1016/j.chom.2020.09.002 (2020).
735 34 Yuan, M. *et al.* Structural basis of a shared antibody response to SARS-CoV-2. *Science*
736 **369**, 1119-1123, doi:10.1126/science.abd2321 (2020).
737 35 Cao, Y. *et al.* Potent Neutralizing Antibodies against SARS-CoV-2 Identified by High-
738 Throughput Single-Cell Sequencing of Convalescent Patients' B Cells. *Cell* **182**, 73-84
739 e16, doi:10.1016/j.cell.2020.05.025 (2020).
740 36 Zhang, Q. *et al.* Potent and protective IGHV3-53/3-66 public antibodies and their
741 shared escape mutant on the spike of SARS-CoV-2. *Nat Commun* **12**, 4210,
742 doi:10.1038/s41467-021-24514-w (2021).
743 37 Weinreich, D. M. *et al.* REGEN-COV Antibody Combination and Outcomes in
744 Outpatients with Covid-19. *N Engl J Med* **385**, e81, doi:10.1056/NEJMoa2108163
745 (2021).
746 38 Gupta, A. *et al.* Early Treatment for Covid-19 with SARS-CoV-2 Neutralizing Antibody
747 Sotrovimab. *N Engl J Med* **385**, 1941-1950, doi:10.1056/NEJMoa2107934 (2021).
748 39 Cohen, M. S. *et al.* Effect of Bamlanivimab vs Placebo on Incidence of COVID-19
749 Among Residents and Staff of Skilled Nursing and Assisted Living Facilities: A
750 Randomized Clinical Trial. *JAMA* **326**, 46-55, doi:10.1001/jama.2021.8828 (2021).
751 40 Group, R. C. Casirivimab and imdevimab in patients admitted to hospital with COVID-
752 19 (RECOVERY): a randomised, controlled, open-label, platform trial. *The Lancet* **399**,
753 665-676, doi:10.1016/s0140-6736(22)00163-5 (2022).
754 41 Levin, M. J. *et al.* Intramuscular AZD7442 (Tixagevimab-Cilgavimab) for Prevention of
755 Covid-19. *N Engl J Med*, doi:10.1056/NEJMoa2116620 (2022).
756 42 Liu, C. *et al.* Reduced neutralization of SARS-CoV-2 B.1.617 by vaccine and
757 convalescent serum. *Cell* **184**, 4220-4236 e4213, doi:10.1016/j.cell.2021.06.020
758 (2021).
759 43 Weissman, D. *et al.* D614G Spike Mutation Increases SARS CoV-2 Susceptibility to
760 Neutralization. *Cell Host Microbe* **29**, 23-31 e24, doi:10.1016/j.chom.2020.11.012
761 (2021).
762 44 Khoury, D. S. *et al.* Neutralizing antibody levels are highly predictive of immune
763 protection from symptomatic SARS-CoV-2 infection. *Nat Med* **27**, 1205-1211,
764 doi:10.1038/s41591-021-01377-8 (2021).
765 45 Feng, S. *et al.* Correlates of protection against symptomatic and asymptomatic SARS-
766 CoV-2 infection. *Nat Med* **27**, 2032-2040, doi:10.1038/s41591-021-01540-1 (2021).
767 46 Harvey, W. T. *et al.* SARS-CoV-2 variants, spike mutations and immune escape. *Nat*
768 *Rev Microbiol* **19**, 409-424, doi:10.1038/s41579-021-00573-0 (2021).
769 47 Lyngse, F. P. *et al.* Transmission of SARS-CoV-2 Omicron VOC subvariants BA.1 and
770 BA.2: Evidence from Danish Households. *medRxiv*, doi:10.1101/2022.01.28.22270044
771 (2022).
772 48 Bruel, T. *et al.* Serum neutralization of SARS-CoV-2 Omicron sublineages BA.1 and
773 BA.2 in patients receiving monoclonal antibodies. *Nat Med*, doi:10.1038/s41591-022-
774 01792-5 (2022).
775 49 Iketani, S. *et al.* Antibody evasion properties of SARS-CoV-2 Omicron sublineages.
776 *Nature*, doi:10.1038/s41586-022-04594-4 (2022).
777 50 Stothard, P. The sequence manipulation suite: JavaScript programs for analyzing and
778 formatting protein and DNA sequences. *Biotechniques* **28**, 1102, 1104,
779 doi:10.2144/00286ir01 (2000).

51 Nakamura, Y., Gojobori, T. & Ikemura, T. Codon usage tabulated from international DNA sequence databases: status for the year 2000. *Nucleic Acids Res* **28**, 292, doi:10.1093/nar/28.1.292 (2000).
52 Tiller, T. *et al.* Efficient generation of monoclonal antibodies from single human B cells by single cell RT-PCR and expression vector cloning. *J Immunol Methods* **329**, 112-124, doi:10.1016/j.jim.2007.09.017 (2008).
53 Ye, J., Ma, N., Madden, T. L. & Ostell, J. M. IgBLAST: an immunoglobulin variable domain sequence analysis tool. *Nucleic Acids Res* **41**, W34-40, doi:10.1093/nar/gkt382 (2013).
54 Lefranc, M. P. IMGT, the International ImMunoGeneTics Information System. *Cold Spring Harb Protoc* **2011**, 595-603, doi:10.1101/pdb.top115 (2011).
55 Katoh, K., Misawa, K., Kuma, K. & Miyata, T. MAFFT: a novel method for rapid multiple sequence alignment based on fast Fourier transform. *Nucleic Acids Res* **30**, 3059-3066, doi:10.1093/nar/gkf436 (2002).
56 Madeira, F. *et al.* The EMBL-EBI search and sequence analysis tools APIs in 2019. *Nucleic Acids Res* **47**, W636-W641, doi:10.1093/nar/gkz268 (2019).
57 Cai, Y. *et al.* Distinct conformational states of SARS-CoV-2 spike protein. *Science* **369**, 1586-1592, doi:10.1126/science.abd4251 (2020).
58 Pettersen, E. F. *et al.* UCSF ChimeraX: Structure visualization for researchers, educators, and developers. *Protein Sci* **30**, 70-82, doi:10.1002/pro.3943 (2021).
59 Goddard, T. D. *et al.* UCSF ChimeraX: Meeting modern challenges in visualization and analysis. *Protein Sci* **27**, 14-25, doi:10.1002/pro.3235 (2018).
60 Dong, E., Du, H. & Gardner, L. An interactive web-based dashboard to track COVID-19 in real time. *The Lancet Infectious Diseases* **20**, 533-534, doi:10.1016/s1473-3099(20)30120-1 (2020).
61 Khare, S. *et al.* GISAID's Role in Pandemic Response. *China CDC Wkly* **3**, 1049-1051, doi:10.46234/ccdcw2021.255 (2021).
62 Elbe, S. & Buckland-Merrett, G. Data, disease and diplomacy: GISAID's innovative contribution to global health. *Glob Chall* **1**, 33-46, doi:10.1002/gch2.1018 (2017).
63 Shu, Y. & McCauley, J. GISAID: Global initiative on sharing all influenza data - from vision to reality. *Euro Surveill* **22**, doi:10.2807/1560-7917.ES.2017.22.13.30494 (2017).

Figure 1

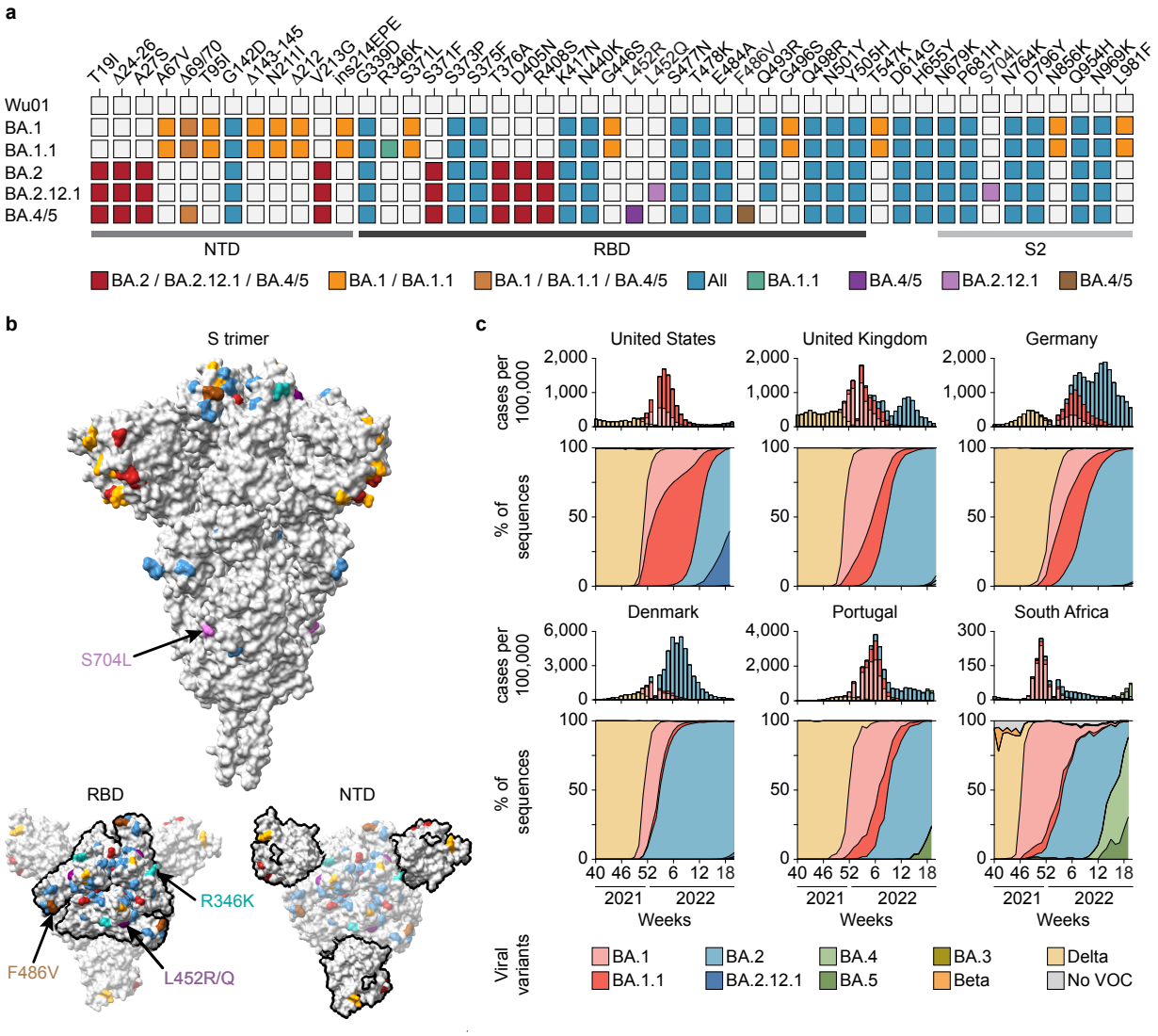

Fig. 1. Omicron sublineage differences.
a, Spike amino acid changes in the BA.1, BA.1.1, BA.2, BA.2.12.1, and BA.4/5 Omicron sublineages relative to Wu01. **b,** Locations of changed amino acids in Omicron sublineages highlighted on the SARS-CoV-2 spike (PDB: 6XR8), with colors indicating mutations shared between different sublineages. Representations at the bottom show RBD and NTD outlined in black. Changes exclusive to BA.1.1 are indicated in green and those to BA.4/5 in brown, residue 452 (mutated in BA.2.12.1 and BA.4/5) is indicated in purple. **c,** Top panels indicate weekly reported SARS-CoV-2 infections as aggregated by the COVID-19 Data Repository by the Center for Systems Science and Engineering at Johns Hopkins University and http://ourworldindata.org. Relative proportions of infections by variant per week were extrapolated from the proportion of sequences submitted to the GISAID SARS-CoV-2 database per variant and week (accessed on May 24, 2022) shown in the bottom panels. NTD, N-terminal domain; RBD, receptor-binding domain; PDB, Protein Data Bank.

Figure 2

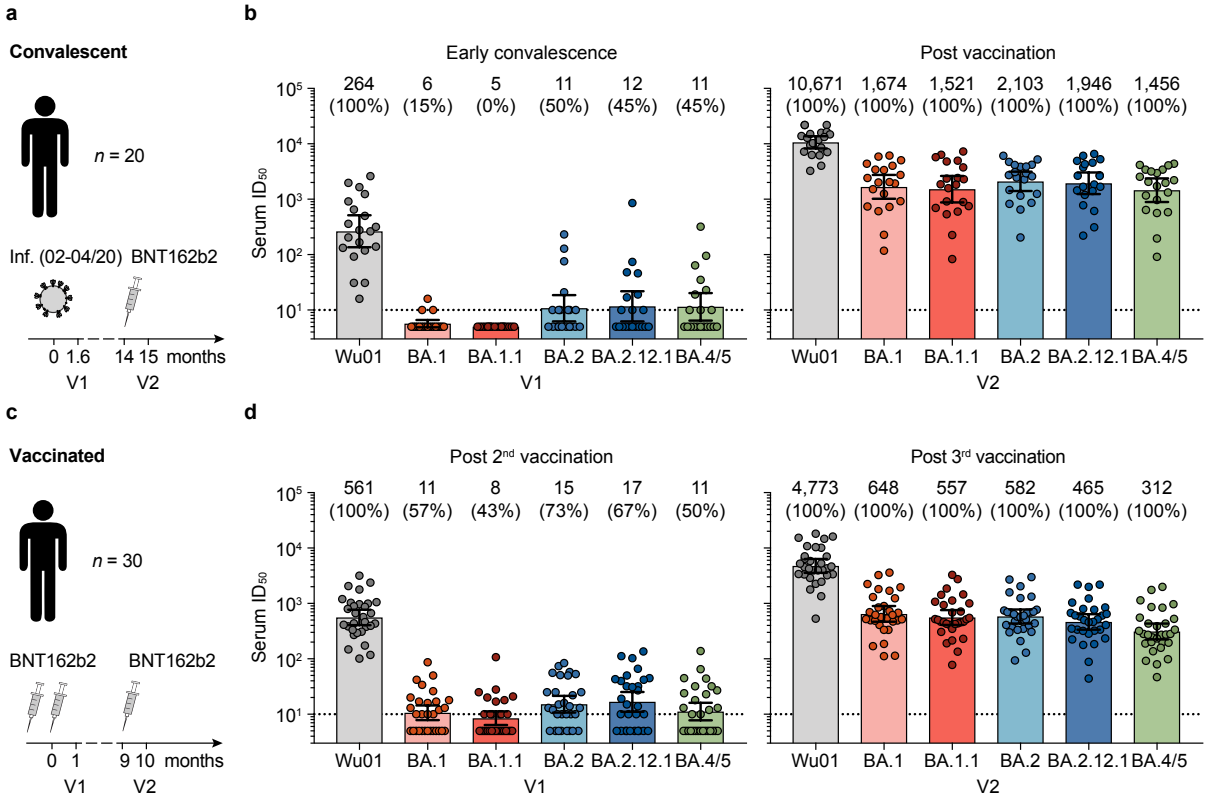

Fig. 2. Omicron sublineage neutralizing serum activity in vaccinated and convalescent individuals.
a, Study scheme in COVID-19-convalescent individuals. Samples were collected after infection occurring between February and April, 2020 (V1), and after a BNT162b2 booster immunization (V2). **b,** Fifty-percent inhibitory serum dilutions (ID_{50}s) against Wu01, BA.1, BA.1.1, BA.2.12.1, and BA.4/5 determined by pseudovirus neutralization assays in convalescent individuals. Bars indicate geometric mean ID_{50}s with 95% confidence intervals (CIs) at V1 (left) and V2 (right). Numbers indicate geometric mean ID_{50}s and percentage of individuals with detectable neutralizing activity (ID_{50} >10) in parentheses. **c,** Study scheme in vaccinated individuals. Samples were collected after the second dose of BNT162b2 (V1) and after the third dose of BNT162b2 (V2). **d,** Serum ID_{50}s against Wu01, BA.1, BA.1.1, BA.2.12.1, and BA.4/5 determined by pseudovirus neutralization assays in vaccinated individuals. Bars indicate geometric mean ID_{50}s with 95% CIs at V1 (left) and V2 (right). Numbers indicate geometric mean ID_{50}s and percentage of individuals with detectable neutralizing activity (ID_{50} >10) in parentheses. In **b** and **d**, ID_{50}s below the lower limit of quantification (LLOQ, ID_{50} of 10; indicated by black dotted lines) were imputed to ½ LLOQ (ID_{50}=5), and ID_{50}s above the upper limit of quantification (21,870) were imputed to 21,871.

Figure 3

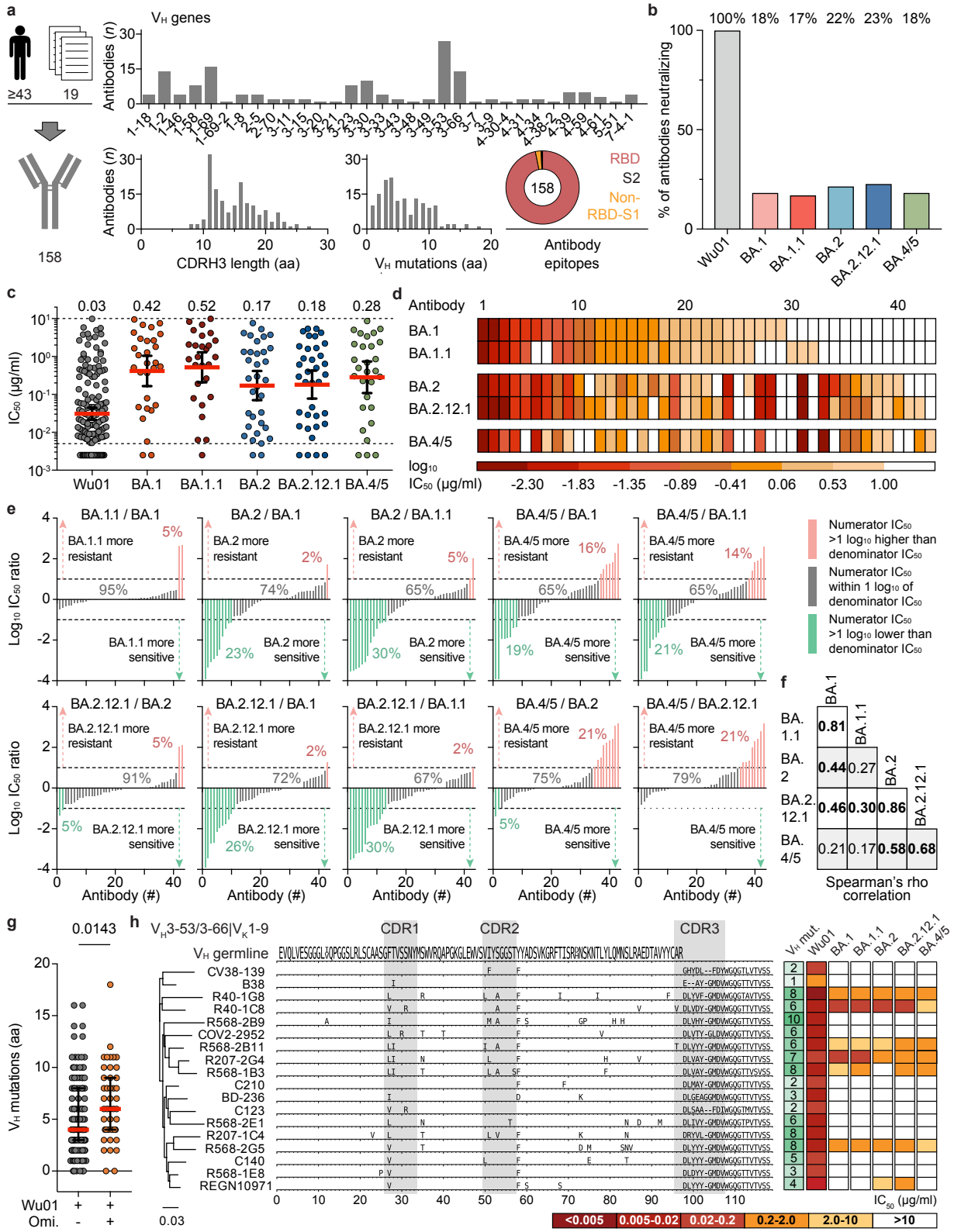

Fig. 3. Determining Omicron sublineage immune escape using monoclonal antibodies.
a, SARS-CoV-2 neutralizing monoclonal antibodies (n=158) derived from 19 studies and ≥43 convalescent individuals were analyzed. Bar charts indicate number of antibodies per heavy chain variable gene segment (V_H), amino acid (aa) length of the heavy chain complementarity-determining region 3 (CDRH3), and number of VH aa mutations relative to the V_H germline gene. Pie chart indicates antibody epitopes with slice sizes proportional to antibody fractions. RBD, receptor-binding domain. **b,** Fractions of antibodies from the panel (n=158) displaying activity (IC_{50} <10 μg/ml) against Wu01 and Omicron sublineages. **c,** IC_{50}s of neutralizing antibodies against individual variants/sublineages (Wu01, n=158; BA.1, n=29; BA.1.1, n=27; BA.2, n=34; BA.2.12.1, n=36; BA.4/5, n=29). Solid lines depict geometric mean IC_{50}s and 95% confidence intervals, and dashed lower and upper lines indicate lower (LLOQ, 0.005 μg/ml) and upper limit of quantification (ULOQ, 10 μg/ml), respectively. IC_{50}s <LLOQ were imputed to ½ LLOQ (IC_{50}=0.0025). **d,** Heat map depicting IC_{50}s of the subset of antibodies (n=43) with neutralizing activity (IC_{50} <10 μg/ml) against at least one of the Omicron sublineages. Antibodies are sorted based on their potency against BA.1. **e,** Log_{10} IC_{50} ratios of antibodies neutralizing any Omicron sublineage for indicated sublineage comparisons. Within each panel, antibodies are sorted by increasing IC_{50} ratios. Ratios <-1 log_{10} are highlighted in green, ratios between -1 and 1 log10 in grey, and ratios >1 log10 in red. Numbers indicate relative fractions. IC_{50} <LLOQ were imputed to ½ LLOQ (IC_{50}=0.0025) and IC_{50} values >ULOQ were imputed to 2x ULOQ (IC_{50}=20). **f,** Spearman's rank correlation coefficients (rho) for comparisons of antibodies with neutralizing capacity against any Omicron sublineage (n=43) as shown in Fig. S2c. Numbers in bold indicate values with p<0.05. **g,** Heavy chain V amino acid mutations of antibodies with neutralizing activity against Wu01 only and antibodies neutralizing both Wu01 and at least one omicron sublineage. Lines indicate medians and interquartile ranges. Groups were compared using the two-tailed Mann-Whitney U test. **h,** Phylogenetic tree and heavy chain sequence alignment of antibodies of the V_H3-53/3-66|V_K1-9 public clonotype. Letters indicate aa mutations relative to the V_H germline gene. Number of aa mutations from corresponding germline allele and neutralizing activity against Omicron sublineages are indicated on the right. Germline V_H represents the consensus of all identified germline alleles of depicted antibodies (V_H3-53*01, V_H3-53*04, and V_H3-66*01). Number of aa mutations from corresponding germline allele and neutralizing activity against Wu01 and Omicron sublineages indicated on the right.

Figure 4

a

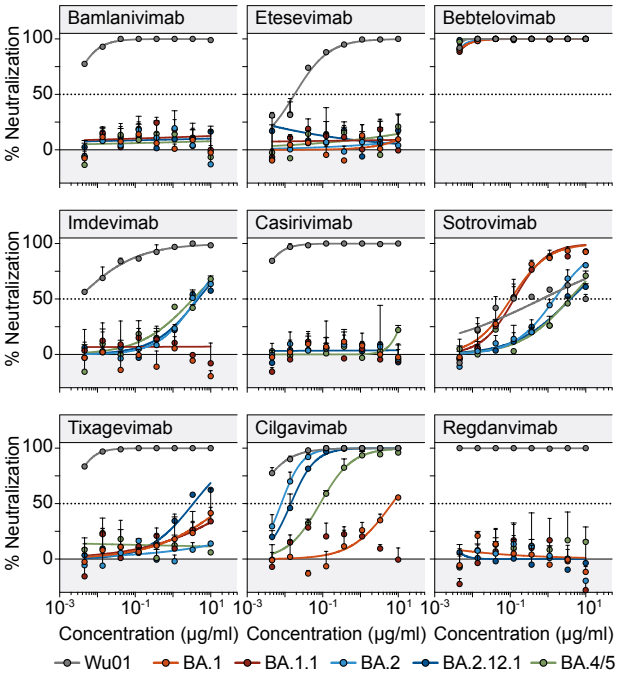

b

	Antibody	IC50 (μg/ml)					
	Name	Wu01	BA.1	BA.1.1	BA.2	BA.2.12.1	BA.4/5
Approved	Bamlanivimab*	<0.005	>10	>10	>10	>10	>10
	Etesevimab*	0.018	>10	>10	>10	>10	>10
	Bebtelovimab†	<0.005	<0.005	<0.005	<0.005	<0.005	<0.005
	Imdevimab*	<0.005	>10	>10	4.173	4.624	3.392
	Casirivimab*	<0.005	>10	>10	>10	>10	>10
	Sotrovimab*	0.976	0.105	0.127	1.488	3.949	3.671
	Tixagevimab†	<0.005	>10	>10	>10	3.438	>10
	Cilgavimab†	<0.005	6.848	>10	0.008	0.014	0.085
	Regdanvimab†	<0.005	>10	>10	>10	>10	>10
In trials	DZIF-10c*	<0.005	0.046	>10	0.033	0.034	8.638
	BRII-196†	0.008	>10	>10	>10	5.398	0.820
	C135†	<0.005	>10	>10	>10	>10	>10
	C144†	<0.005	>10	>10	>10	>10	>10
	COV2-2381†	0.008	>10	>10	>10	>10	>10
	ADG-2†	<0.005	0.212	0.194	>10	>10	>10
	47D11†	0.386	>10	>10	>10	>10	>10
	BD-368-2†	<0.005	>10	>10	>10	>10	>10
	MAD0004J08†	<0.005	>10	>10	>10	>10	>10

Monoclonal antibody used for neutralization assay:
* Clinical product used.
† Parental antibody (Fc-unmodified IgG1) used.

c

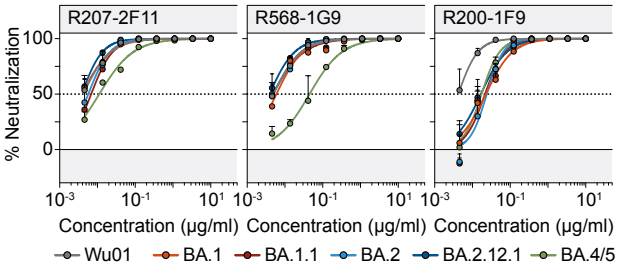

d

Antibody	IC50 (μg/ml)					
Name	Wu01	BA.1	BA.1.1	BA.2	BA.2.12.1	BA.4/5
R207-2F11	<0.005	<0.005	0.006	0.006	<0.005	0.011
R568-1G9	0.007	0.006	0.006	0.005	<0.005	0.045
R200-1F9	<0.005	0.023	0.025	0.026	0.017	0.017
	B.1	Alpha	Beta	Delta	Epsilon	Kappa
R207-2F11	0.003	0.004	0.013	0.004	0.002	0.011
R568-1G9	0.002	0.003	0.001	0.002	0.002	0.006
R200-1F9	0.001	0.002	0.002	0.004	0.003	0.003

Fig. 4. Omicron sublineage neutralizing activity of monoclonal antibodies in clinical use.
a, Dose response curves showing percentage neutralization of monoclonal antibodies against Wu01 and Omicron sublineages in pseudovirus neutralization assay. Circles show averages and error bars indicate standard deviation. Dotted lines indicate 50% neutralization (IC_{50}). **b,** IC_{50}s of monoclonal antibodies with current or previous authorization for clinical use or in clinical development. Symbols indicate whether clinical products or parental antibodies produced as human IgG1 were used. **c,** Dose response curves showing percentage neutralization of novel monoclonal antibodies against Wu01 and Omicron sublineages in pseudovirus neutralization assay. Circles show averages and error bars indicate standard deviation. Dotted lines indicate 50% neutralization (IC_{50}). **d,** IC_{50}s of novel monoclonal antibodies shown in **c** against Wu01 and Omicron sublineages (upper rows) and previously circulating variants (lower rows, as previously determined[30]).